Efficient cooperative transmissions with dynamic clustering in realistically designed small cells

Panagiotis Georgakopoulos, Tafseer Akhtar, Christos Tselios, Ilias Politis
Wireless Communications Laboratory,
University of Patras, Greece
{pgeorgako, tselios, ipolitis}@ece.upatras.gr, akhtar@upatras.gr

***Abstract*—Modern wireless networks promise high performance and quality of service to the ever-growing number of mobile users. However, limited radio resources, high interference and poor channel conditions are significant obstacles for reliable and high quality service provision. To tackle these issues, a scheme where JT-CoMP is deployed in a Cloud Radio Access Network (C-RAN) small cell topology is proposed, where the clustering of the remote radio heads (RRHs) is based on a dynamic coalition formation algorithm. To obtain more reliable and accurate results of the JT-CoMP deployment, TruNET wireless was used alongside Vienna LTE-A Downlink System Level Simulator to model the propagation environment. To test our proposed scheme's performance, the throughput of immobile and high-speed moving users is examined in separate scenarios.**

***Index Terms*—5G, C-RAN, coalition formation games, coordinated multipoint, interference coordination, radio resource management, small cells**

I. Introduction

Fifth generation (5G) networks are in their deployment phase and are expected to efficiently support [1] a large number of devices with a huge network traffic demand and multiple demanding usage scenarios including Enhanced Mobile Broadband (eMBB), Ultra-Reliable and Low Latency Communications (URLLC) and Massive Machine-Type Communications (mMTC) [2]. To achieve this, increased system capacity has to be provided alongside with techniques to guarantee a reliable low-latency service provision and high Quality of Experience (QoE) [3].

A key mechanism to increase capacity is the network densification, where cells of small coverage are deployed in high traffic indoors and outdoors areas, creating a dense network of small cells, while ensuring nearly uniform distribution of users among all cells [4]. However, a dense small cell deployment means that, compared to a macro cell network, the number of interfering non-serving cells for mobile user equipments (UEs) is increased, while the distance between them is decreased, resulting in high intercell interference, especially for users located in cell edges.

To address this issue, Joint Transmission Coordinated Multipoint (JT-CoMP) can be implemented in the system. JT-CoMP is an advanced CoMP scheme where the same resource block (RB) of the PDSCH can be transmitted from multiple transmission points to coherently or non-coherently improve the received signal quality and throughput [5]. Therefore, in JT-CoMP the intercell interference can be mitigated by converting an interfering signal from another cell to a desired signal. However, JT-CoMP requires the transmitted data to be available at all the cooperating transmission points, stressing the backhaul links. Also, the scheduling and processing complexity increases with the number of cooperating transmission points [6].

To enable the small cell deployment and JT-CoMP, Cloud Radio Access Networks (C-RAN) can be considered. The main idea behind C-RAN is to separate the radio unit, i.e. the remote radio head (RRH) from the baseband unit (BBU) while centralizing the baseband processing in a virtualized baseband unit (BBU) pool [7]. C-RAN can severely reduce the small cell realization cost by lowering the number of BBUs in densely deployed heterogeneous small cell networks and enhance their energy efficiency while reducing their power consumption. Regarding JT-CoMP, C-RAN can efficiently support its implementation as multiple BBUs can coordinate with each other to share the scheduling information, channel status and user data efficiently to improve the system capacity as well as reduce interferences in the system [8].

The clustering of cooperating transmission points in JT-CoMP has been identified as a significant challenge in various studies [9], [10]. As shown in our previous studies [11], [12], incautious clustering can result in reduced spectral efficiency and data rates for the UEs not in the cell edges (or non-edge UEs) as there is a high probability of committing too many resources to cell edge UEs (or edge UEs), especially if their percentage in the network is high. Also, JT-CoMP stresses the links between the BBU pool and the core network, i.e. the backhaul links. A game theoretic approach based on coalition formation games can address these issues. Coalition formation games account for network structure and the costs of cooperation, while satisfying the individual rational demands of the network nodes [13], which is why clustering in this study is based on this method.

Our previous works [11], [12] examine the performance of JT-CoMP in a C-RAN small cell scenario with a backhaul constraint and variable number of deployed RRHs, where the UEs are assumed still for the duration of the proposed coalition formation algorithm. Vienna LTE-A Downlink System Level Simulator [14] was used for realizing the simulations. The proposed scheme's performance in terms of edge and non-edge

978-1-7281-6339-0/20/$31.00 ©2020 IEEE

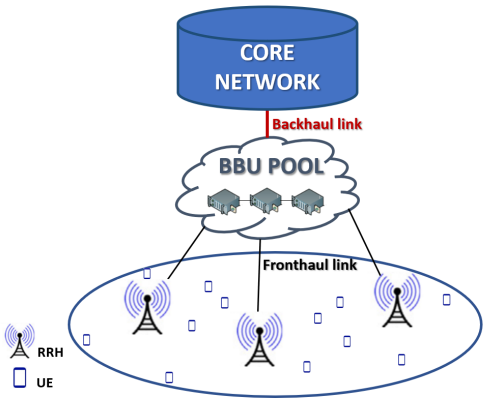

Fig. 1: C-RAN small cell network architecture.

UE throughput is compared with that of a conventional JT-CoMP scenario where the JT-CoMP clusters are predetermined based on the distance between interfering RRHs and a scenario where JT-CoMP is not deployed.

In this study, the performance and adaptability of a modified version of the proposed algorithm of [11], [12] is tested in a scenario where a high-speed user is moving between cells, activates handovers and changes the involved cells' load. Furthermore, we enhance the simulation accuracy capabilities of LTE-A Downlink System Level Simulator by importing physical layer parameters from TruNET wireless [15]. This study is organized as follows. In Section II the system model will be presented, while in Section III the coalition formation game will be defined. In Section IV, the proposed coalition formation game will be analyzed. Finally, in Section V the simulation setup and the results are presented and discussed, followed by the conclusions in Section VI.

Regarding notations, we will use lowercase or uppercase letters for scalars, boldface lowercase letters for vectors, boldface uppercase letters for matrices. Furthermore, the superscripts $(\cdot)^T$, $(\cdot)^H$, $(\cdot)^{-1}$, $(\cdot)^\dagger$ denote the transpose, the conjugate transpose, the matrix inverse and the Moore-Penrose pseudo-inverse respectively. Additionally, $|\cdot|$ and $||\cdot||$ indicate the norm and the Euclidean norm of a scalar and vector respectively.

II. System Model

A homogeneous C-RAN based small cell network consisting of L RRHs in the access network is assumed, where OFDMA is the selected multiple access scheme and the RRHs are assumed to have omnidirectional coverage, forming L total cells. We focus on the downlink transmission where the L total RRHs of the network serve a total of K UEs each, accounting for $L \cdot K$ total UEs in the network. The available frequency spectrum is divided into R subcarriers, while in every Transmission Time Interval (TTI) each RRH has R Resource Blocks (RBs) available to serve its attached UEs. The model of the considered system architecture is illustrated in Fig. 1.

Let $\mathcal{L} = \{1,\ldots,l,\ldots,L\}$ represent the set of RRHs, while $\mathcal{K} = \{1,\ldots,k,\ldots,K\}$ represents the set of each cell's UEs. All the UEs are equipped with N_r antennas, while the RRHs are equipped with N_t omnidirectional antennas.

Prior to the transmission over the wireless channel, the user symbol vector $\boldsymbol{x}_{k,l,r}$ is precoded with a precoding matrix $\boldsymbol{W}_{k,l,r} \in \mathbb{C}^{N_t \times n_{k,l}}$, mapping the $n_{k,l}$-dimensional transmit symbol vector onto the N_t antennas, where $n_{k,l}$ is the number of data-streams spatially multiplexed to user k, with $n_{k,l} \leq \mathrm{N_r}$. Also, the allocation of the available transmit power is considered in the precoding matrices.

For the r-th subcarrier, the N_r-dimensional received signal vector of UE k, served by RRH l can be expressed by the following formula:

$$\boldsymbol{r}_{k,l,r} = \boldsymbol{H}_{k,l,r}\boldsymbol{W}_{k,l,r}\boldsymbol{x}_{k,l,r} + \sum_{i=1,\neq l}^{L} \boldsymbol{H}_{k,i,r}\boldsymbol{W}_{s,i,r}\boldsymbol{x}_{s,i,r} + \boldsymbol{z}_{k,l,r} \tag{1}$$

where, $\boldsymbol{H}_{k,l,r} \in \mathbb{C}^{N_r \times N_t}$ is the total MIMO channel matrix describing the channel between UE k and RRH l and $\boldsymbol{z}_{k,l,r} \in \mathcal{N}_{\mathbb{C}}\left(0, \sigma_z^2 I_{N_r}\right)$ is the Additive White Gaussian Noise (AWGN) added at the receiver. The second term of the equation (1) represents the intercell interference caused by transmissions from other RRHs in the network (noted i) to other UEs (noted s) at the r-th subcarrier. Also, it is assumed that the transmit symbol vector is normalized as:

$$\mathbb{E}\left[\boldsymbol{x}_{k,l,r}\boldsymbol{x}_{k,l,r}^H\right] = \boldsymbol{I}_{n_{k,l}} \tag{2}$$

where, $\boldsymbol{I}_{n_{k,l}}$ is the identity matrix sized $n_{k,l}$.

The users are assumed to employ a zero-forcing filter to equalize their respective channels and to separate spatially multiplexed data-streams from each other and from the interference caused by transmissions to other users. The $n_{k,l} \times N_r$ dimensional receive filtering matrix applied to user k in cell l, is denoted as $\boldsymbol{G}_{k,l,r}$. Applying this matrix to the received signal vector, the estimated symbol vector is obtained as:

$$y_{k,l,r} = \boldsymbol{G}_{k,l,r}\boldsymbol{H}_{k,l,r}\boldsymbol{W}_{k,l,r}\boldsymbol{x}_{k,l,r} + \sum_{i=1,\neq l}^{L} \boldsymbol{G}_{k,l,r}\boldsymbol{H}_{k,i,r}\boldsymbol{W}_{s,i,r}\boldsymbol{x}_{s,i,r} + \boldsymbol{z}_{k,l,r} \tag{3}$$

The ZF receive filter is expressed as:

$$\boldsymbol{G}_{k,l,r} = \left((\boldsymbol{\Gamma}_{k,l,r})^H \boldsymbol{\Gamma}_{k,l,r}\right)^{-1} (\boldsymbol{\Gamma}_{k,l,r})^H \tag{4}$$

where,

$$\boldsymbol{\Gamma}_{k,l,r} = \boldsymbol{H}_{k,l,r}\boldsymbol{W}_{k,l,r} \tag{5}$$

Assuming the described zero-forcing filter on the receiver side, the post equalization SINR for the k-th UE which is served by the l-th RRH, for the stream $v \in [1,\ldots, n_{k,l}]$, at the r-th subcarrier is expressed by the following formula:

$$SINR_{k,l,r,v} = \frac{\left|\boldsymbol{g}_{k,l,r,v}^H \boldsymbol{H}_{k,l,r}\boldsymbol{w}_{k,l,r,v}\right|^2}{I_{intercell} + I_{self} + \sigma_z^2\left|\boldsymbol{g}_{k,l,r,v}\right|^2} \tag{6}$$

where,

$$I_{intercell} = \sum_{i=1,\neq l}^{L} |\boldsymbol{g}_{k,l,r,v}^{H} \boldsymbol{H}_{k,i,r} \boldsymbol{W}_{s,i,r}|^2 \quad (7)$$

$$I_{self} = \sum_{\mu=1,\neq v}^{n_{k,l}} |\boldsymbol{g}_{k,l,r,v}^{H} \boldsymbol{H}_{k,l,r} \boldsymbol{w}_{k,l,r,\mu}|^2 \quad (8)$$

At equations (6)-(8), $\boldsymbol{g}_{k,l,r,v}$ and $\boldsymbol{w}_{k,l,r,v}$ denote the v-th column of $\boldsymbol{G}_{k,l,r}^{H}$ and $\boldsymbol{W}_{k,l,r}$ respectively. The useful signal power of stream v is represented by the numerator, while the denominator includes the intercell interference power from other RRHs that operate at the same frequency, given by equation (7), self-interference caused by other user streams, given by equation (8), and the noise power. The symbols of different users are assumed as statistically independent. Single User Multiple Input Multiple Output (SU-MIMO) is assumed, so the interference between the spatially multiplexed streams is ignored on the formulas.

After the per-subcarrier and per-stream post equalization SINR is extracted, MIESM (Mutual Information Effective Signal to Interference and Noise Ratio Mapping) [16] is employed to calculate an effective SINR value via compressing the corresponding post equalization SINR values of the assigned RBs, yielding an AWGN-equivalent representation in terms of mutual information, in order to determine the CQI and the MCS. This single effective SINR value is then be further mapped to a BLER (Block Error Ratio) value. After that, the size of the Transport Block can be determined according to the LTE standards and an instantaneous throughput value can be obtained for the current TTI.

The UEs are divided into two categories based on their effective SINR, edge and non-edge UEs. For a non-edge user, the previously described equations apply for their post equalization SINR and throughput calculation. When a UE is considered edge, it can be served by multiple cooperating RRHs which can form a JT-CoMP coalition Π_s. We define $\mathcal{P}$ = $\{\Pi_1, \Pi_2, \ldots, \Pi_s, \ldots, \Pi_S\}$ as the set of coalitions in the network. In this case, the composite total channel matrix $\boldsymbol{H}_{k,l,r}$ is calculated by stacking the matrices from each transmitter $c \in [1, \ldots, C]$ in the coalition, as in [17], i.e.,

$$\boldsymbol{H}_{k,l,r} = [\boldsymbol{H}_{k,l_1,r}, \ldots, \boldsymbol{H}_{k,l_C,r}] \, \epsilon \mathbb{C}^{N_r \times CN_t} \quad (9)$$

Then, the per-subcarrier and per-stream post equalization SINR for edge UE k_e which is served by a coalition Π_s is expressed by the following equation:

$$SINR_{k,l,r,v} = \frac{\left| \boldsymbol{g}_{k_e,l,r,v}^{H} \boldsymbol{H}_{k_e,l,r} \boldsymbol{w}_{k_e,l,r,v} \right|^2}{I_{intercell} + I_{self} + \sigma_z^2 \left| \boldsymbol{g}_{k_e,l,r,v} \right|^2} \quad (10)$$

where,

$$I_{intercell} = \sum_{i=1,\notin \Pi_s}^{L} |\boldsymbol{g}_{k_e,l,r,v}^{H} \boldsymbol{H}_{k_e,i,r} \boldsymbol{W}_{s,i,r}|^2 \quad (11)$$

$$I_{self} = \sum_{\mu=1,\neq v}^{n_{k,l}} |\boldsymbol{g}_{k_e,l,r,v}^{H} \boldsymbol{H}_{k_e,l,r} \boldsymbol{w}_{k_e,l,r,\mu}|^2 \quad (12)$$

Then, an effective SINR value is extracted using MIESM and the throughput of the edge UE is calculated based on the LTE specifications.

III. Problem formulation

In this section, the proposed coalition formation game will be defined and formulated.

It is evident by observing equations (10)-(12) that the more RRHs in a coalition, the more the numerator of equation (10) increases, while the denominator decreases, resulting in a higher SINR value for an edge UE which can be translated to higher throughput. This is a strong incentive for RRHs to form coalitions and coordinate their transmissions with JT-CoMP. However, by implementing JT-CoMP, some RBs from each cooperating RRH will be assigned to the edge UEs of the cluster instead of their attached non-edge UEs. This can potentially decrease severely their throughput. Coalition formation games account for cooperation costs [13], therefore they are suitable to address this problem.

Our goal is to formulate a problem where an RRH decides to participate in a coalition only when the throughput of all its edge UEs improves, the throughput of its non-edge UEs does not decrease severely and the backhaul links are not stressed beyond a threshold. Therefore, a coalition formation game with non-transferable utility (NTU), defined by a pair $(\mathcal{L}, U)$, where $\mathcal{L}$ presents the finite set of players and U as a characteristic function which associates with every coalition $\Pi_s \subseteq \mathcal{L}$ a set of payoff vectors, where:

$$U(\Pi_s) = \begin{cases} V(\Pi_{cl}) & , T \leq T_{thres} \\ 0 & , T \geq T_{thres} \end{cases} \quad (13)$$

where T_{thres} is the backhaul capacity threshold and is calculated as in [18] and:

$$V(\Pi_s) = \sum_{l \in \Pi_i} x_l(\Pi_s) \quad (14)$$

Additionally we define a partition B of $\mathcal{L}$, as a collection $\mathcal{P}$ of coalitions encompassing all the players of $\mathcal{L}$. The individual payoff $x_l(\Pi_s)$ of RRH l participating in coalition Π_s can be expressed as:

$$\begin{aligned} x_l(\Pi_s) = A_l - (E_l - 1 - q_{e,l} + \beta_{e,l}) \\ - (N_l - 1 - q_{n,l} + \beta_{n,l}) + x_l' \end{aligned} \quad (15)$$

and

$$A_l = \sum_{k_e=1}^{E_l} sgn(R_{k_e,l} - R'_{k_e,l}) + \sum_{k_n=1}^{N_l} sgn(R_{k_n,l} - d_f R'_{k_n,l}) \quad (16)$$

where, d_f $(0 \leq d_f \leq 1)$ represents the acceptable percentage of non-edge UE throughput that remains after a coalition is

tested, E_l and N_l denote the total number of edge and non-edge UEs attached to RRH l, $R_{k_e,l}$ and $R_{k_n,l}$ represent the throughput of an edge and non-edge UE respectively after the coalition Π_s is formed and JT-CoMP is activated. Intonations were used for values of previous partitions that satisfied the game's conditions and $R'_{k_n,l}$ is always the throughput of non-edge UE k_n before the game starts. Also, $q_{e,l}$ and $q_{n,l}$ account for the number of edge and non-edge UEs respectively with intact throughput before and after Π_s is tested, while $\beta_{e,l}$ and $\beta_{n,l}$ represent the number of edge and non-edge UEs with decreased throughput after Π_s. Finally, in equation (16) the signum function was used.

Equations (15) and (16) were formulated in a way that if at least one of the examined cluster's RRHs's edge UE's throughput decreased or at least one of its non-edge UE's throughput decreased below its corresponding threshold, the payoff of the RRH decreases which will lead to the rejection of the examined coalition. In the opposite case, the coalition will be formed as long as the backhaul constraint is satisfied. Therefore, the coalition formation game can be played by the RRHs on behalf of its attached UEs.

IV. Proposed coalition formation algorithm

In this section, the proposed coalition formation algorithm for the self organization of the RRHs in coalitions will be introduced. We assume that mobile users can move for the duration of the game. This imposes changes to the game's nature, as moving UEs can be attached to different RRHs by activating handovers while changing their traffic load. Moreover, propagation channels are dynamic, resulting in varied effective SINRs for the UEs, which can cause changes in their edge or non-edge status. Therefore, a dynamic coalition formation algorithm needs to be constructed that can adapt to possible changes. Our proposed algorithm is a modified version of the coalition formation algorithm based on merge and split operations in [11], [12] and is divided in three stages:

1) **Stage I**: Initially, the network consists of $L \in \mathcal{L}$ players, referred to as singleton coalitions.
2) **Stage II**: In the second stage, each edge UE forwards to the cloud a carrier-to-interference (C/I) vector containing C/I values from each interfering RRH through its serving RRH. If an RRH serves more than one edge UEs, then the cloud averages the values of their C/I vectors and merges them into a single vector. After that, the vectors are sorted in ascending order and unitize to create an $(L-1) \times L$ C/I matrix.
3) **Stage III**: In the third stage, a repeated procedure is performed, where each row of the C/I matrix is extracted, its C/I values are sorted, and if they do not exceed a predetermined C/I threshold, a priority and cooperation candidate list are created. These lists indicate the order that possible coalitions are going to be tested. For an examined coalition, if a player improves its payoff, while the payoff of the others is at least not reduced and the utility of the coalition increases as well, then the coalitions merge. A formed coalition will split only if at least one RRH in that coalition is able to strictly improve its individual payoff via split operation without decreasing the payoff of the rest. To improve accuracy and capture possible changes in UE effective SINR due to mobility and channel variations, each iteration of the game is run for a fixed time duration where JT-CoMP is activated. The proposed algorithm can be reactivated when a handover occurs or when a non-edge UE becomes edge and vice versa, unless it is already running.

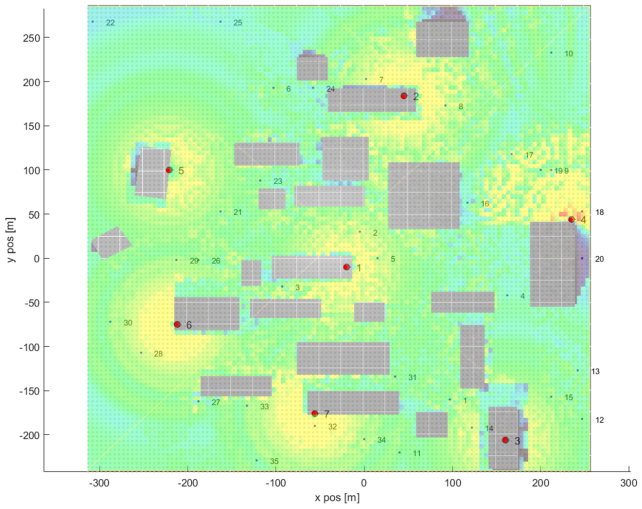

Fig. 2: Network topology with received power mapping using TruNET wireless.

To decide whether a merge or split will occur, we compare coalitions based on the Pareto order which means that a partition B_1 is preferred over B_2 if at least one player in B_1 improves its payoff via participating in a coalition Π_s without hurting the throughput of the other players [19].

It is proven in [19] that any iteration of successive arbitrary merge and split operations terminates. Also, the C/I threshold ensures that the proposed algorithm will converge in a limited number of steps, as only the stronger interferers of each RRH are taken into account. Moreover, this ensures that the UEs' channel gains will not drastically change over the duration of the proposed algorithm. Also, the proposed algorithm's complexity is $O(L_n)$, where L_n is the average number of neighbouring RRHs that create significant interference to each RRH. Finally, a network partition B resulting from the proposed coalition formation algorithm can no longer be subject to any additional merge or split operations as successive iterations of these operations terminate [19]. Therefore, the users in the final network partition cannot leave this partition through merge and split and the partition is immediately $\mathbb{D}_{hp}$-stable.

V. Performance analysis

A. Simulation setup

A C-RAN based small cell network consisting of 7 RRHs, each serving 5 UEs, is considered where the propagation topol-

ogy is modeled after the University of Patras campus. Each RRH forms a small cell, is assumed to have omnidirectional coverage and is equipped with two antennas, whilst every UE is equipped with 2 receive antennas. The effective SINR threshold that determines whether a user is considered edge or non-edge was set at 3 dB. A carrier frequency of 2.14 GHz and a transmission power of 1 Watt was assumed. Finally, each RRH had 20 MHz of available bandwidth, resulting into 100 RBs available for transmission at every TTI, according to the LTE-A specifications.

TABLE I: Simulation Parameters

Parameter description	Value
Carrier frequency	2.14 GHz
Num. of RRHs	7
Num. of UEs per RRH	5
Inter-RRH distance	varied
Transmit power	1 Watt
Transmitter height	varied
Receiver height	1.5 meters
Antenna gain pattern	Omni-directional
Max Tx antenna gain	17 dBi
Rx antenna gain	0 dBi
Number of Tx antennas	2
Number of Rx antennas	2
LTE transmission mode	CLSM
Channel model	Typical Urban
Receiver type	Zero-forcing
Feedback delay	1 TTI
Bandwidth	20 MHz
Receiver noise figure	9 dB
Thermal noise density	-174 dBm/Hz

We focus on two use cases. In the first one, TruNET wireless link layer parameters can be imported in Vienna LTE-A Downlink System Level Simulator. The case where these parameters are imported is referred to as the active integration case, otherwise the integration is inactive. Then, the performance of the edge UEs, in terms of throughput, in both JT-CoMP with coalition formation algorithm, referred to as game JT-CoMP, and non JT-CoMP scenarios are compared with each other for the cases that the integration is active or inactive. TruNET wireless is a realistic 3D polarimetric physical layer simulator capable of accurately simulating radio propagation effects in urban and suburban scenarios based on advanced ray tracing techniques. Therefore, its use alongside Vienna LTE-A Downlink System Level Simulator enables the accurate study of our proposed scheme's impact in any scenario. When the integration is active, the shadow fading and path loss parameters are imported from TruNET wireless, otherwise Vienna LTE-A System Level Simulator provides these values. In this use case, the UEs are considered immobile for the duration of the simulations. The simulation topology along with the received power mapping in the propagation environment, provided by TruNET wireless, are presented in Fig. 2.

In the second use case, the throughput of a moving edge UE is examined for the game JT-CoMP and no JT-CoMP case, as it is moving between two predetermined points. The moving UE can activate handovers, meaning that after a handover its newly attached RRH will serve 6 UEs, including the moving user. The speed of the UE was set at 100 km/h. Again, the shadowing and path loss parameters are imported from TruNET wireless.

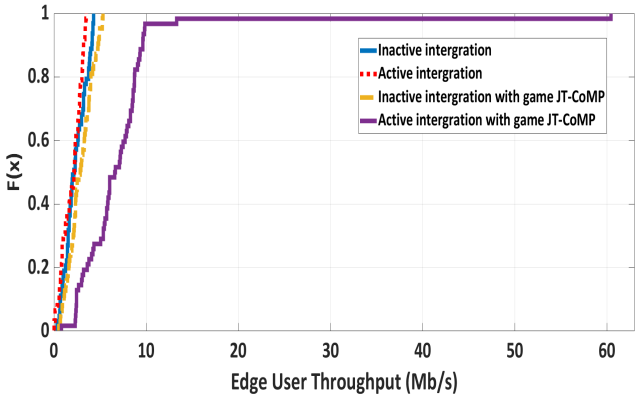

Fig. 3: CDF of edge user throughput

TABLE II: Description of moving UE's status, serving RRH(s) and the algorithm's activation for all the simulation runs.

Execution Round(s)	Serving RRH(s)	Algorithm	Status
1	1	inactive	edge
2-28	1,4	active	edge
29-33	1,4	inactive	edge
33 + 9 TTIs (Handover)	5	inactive	edge
34-42	5,2	active	edge
43-58	5,2	inactive	edge
58-95	5	inactive	non-edge
96-113	5,2	active	edge
113-116	5,2	inactive	edge
116 + 9 TTIs (Handover)	4	active	edge
117-129	4,1,5,2	active	edge
129-149	4,1,5,2	inactive	edge

For all simulations, the backhaul capacity threshold was set at 500 Mb/s and the C/I threshold at 10 dB. Also, the Typical Urban (TU) PDP profile was used for the computation of the small-scale parameters. Each iteration of the algorithm that decides a merge or split was run for 10 TTIs, while d_f was set at 0.5. A summary of the simulation parameters is presented in Table I. A total of 100 simulations per use case were run for increased accuracy. A conventional case for JT-CoMP deployment, e.g. with static coalitions based on distance, was not examined, as it was presented and analyzed at [11].

B. Results

Fig. 3 presents the CDF of the edge UEs' throughput when the integration is active versus the case its inactive, with and without game JT-CoMP implementation. As expected, JT-CoMP improves the edge UEs' throughput whether the integration is active or not. The impact of TruNET wireless is obvious as the throughput values of the UEs are different for both the non JT-CoMP and JT-CoMP case. This difference certifies the gain of implementing deterministic parameters for

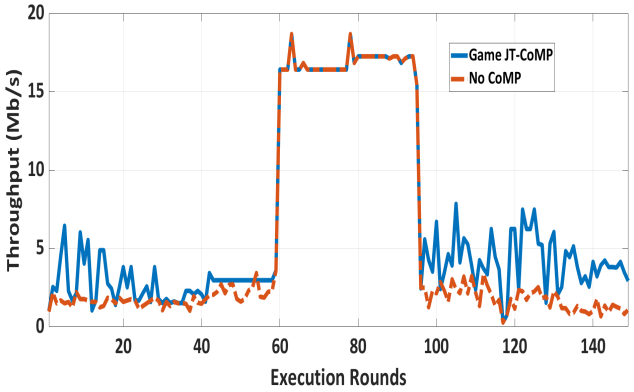

Fig. 4: Moving user average throughput per execution round

simulations which can transform them into extremely reliable and accurate network planning tools.

Fig. 4 depicts the average throughput per 10 TTIs for an user (UE 4 at Fig. 2) moving at 100 km/h speed between two predetermined points when game JT-CoMP is activated versus the case it is not. Also, Table II provides a detailed description of the number of serving RRHs, the UE's status and the execution rounds that the algorithm was activated throughout the user's movement. We assume that 10 TTIs correspond to an execution round and that the integration is active. At the first execution round, the UE acquired its edge status and the algorithm activated until execution round 28. After a handover during execution round 39, the UE was momentarily served by one RRH before the proposed coalition formation algorithm was activated again and the UE was served by two cooperating RRHs. At execution round 58 the UE was considered non-edge, so it was not served by a coalition. The user regained its edge status at execution round 96, the coalition formation algorithm was reactivated and the user was served by a coalition via JT-CoMP. Again, after a handover at execution round 116, our proposed algorithm was activated again and this time a larger coalition was formed to serve the moving UE. By observing Fig. 4, it is clear that game JT-CoMP was beneficial for the UE's throughput and it was able to quickly assign cooperating RRHs for its service, despite handovers and status changes.

VI. Conclusions

The needs of users in modern wireless networks impose significant challenges in terms of network capacity and reliable provision of multiple services. Limited radio resources, poor channel conditions and intercell interference due to edge cell positioning can endanger the high QoE for multiple UEs in the network. A dynamic coalition formation game was formulated in order to form the most beneficial coalitions for implementing JT-CoMP, to mitigate intercell interference and serve the network's users with poor wireless links.

By implementing our proposed scheme, we enhance the system with self organization elements, as the system is capable of forming the most beneficial transmission point coalitions to cope with interference and network structure changes due to user mobility or bad channel conditions. Simulations, enhanced with deterministically computed channel parameters, shown that whether the examined users were moving or not, the proposed coalition formation algorithm along with JT-CoMP were able to improve their throughput.

Acknowledgment

This research was funded by the Research Project SONNET H2020-MSCA-RISE-2016-SONNET-734545 and SECRET (H2020-MSCA-ITN-2016 SECRET-722424).

References

[1] Mumtaz, Shahid, et al. "Self-organization towards reduced cost and energy per bit for future emerging radio technologies-sonnet." 2017 IEEE Globecom Workshops (GC Wkshps). IEEE, 2017.
[2] Navarro-Ortiz, Jorge, et al. "A survey on 5G usage scenarios and traffic models." IEEE Communications Surveys & Tutorials (2020).
[3] Pierucci, Laura. "The quality of experience perspective toward 5G technology." IEEE Wireless Communications 22.4 (2015): 10-16.
[4] Bhushan, Naga, et al. "Network densification: the dominant theme for wireless evolution into 5G." IEEE Communications Magazine 52.2 (2014): 82-89.
[5] Sawahashi, Mamoru, et al. "Coordinated multipoint transmission/reception techniques for LTE-advanced [Coordinated and Distributed MIMO]." IEEE Wireless Communications 17.3 (2010): 26-34.
[6] Lee, Daewon, et al. "Coordinated multipoint transmission and reception in LTE-advanced: deployment scenarios and operational challenges." IEEE Communications Magazine 50.2 (2012): 148-155.
[7] Checko, Aleksandra, et al. "Cloud RAN for mobile networks—A technology overview." IEEE Communications surveys & tutorials 17.1 (2014): 405-426.
[8] Mobile, China. "C-RAN: The road towards green RAN, white paper, ver. 2.5." China Mobile Research Institute (2011).
[9] Irmer, Ralf, et al. "Coordinated multipoint: Concepts, performance, and field trial results." IEEE Communications Magazine 49.2 (2011): 102-111.
[10] Jungnickel, Volker, et al. "The role of small cells, coordinated multipoint, and massive MIMO in 5G." IEEE communications magazine 52.5 (2014): 44-51.
[11] Georgakopoulos, Panagiotis, Tafseer Akhtar, and Stavros Kotsopoulos. "On Game Theory-Based Coordination Schemes for Mobile Small Cells." 2019 IEEE 24th International Workshop on Computer Aided Modeling and Design of Communication Links and Networks (CAMAD). IEEE, 2019.
[12] Georgakopoulos, Panagiotis, et al. "Coordination Multipoint Enabled Small Cells for Coalition-Game-Based Radio Resource Management." IEEE Network 33.4 (2019): 63-69.
[13] Han, Zhu, and H. Vincent Poor. "Coalition games with cooperative transmission: a cure for the curse of boundary nodes in selfish packet-forwarding wireless networks." IEEE Transactions on Communications 57.1 (2009): 203-213.
[14] Rupp, Markus, Stefan Schwarz, and Martin Taranetz. The Vienna LTE-advanced simulators. Singapore: Springer, 2016.
[15] TruNET Wireless. Available online: http://www.fractalnetworx.com
[16] Alexiou, Angeliki, et al. "IST-2003-507581 WINNER D2. 7 ver 1.0 Assessment of Advanced Beamforming and MIMO Technologies." Information Society Technologies, Belgium, Tech. Rep. (2005).
[17] Taranetz, Martin, et al. "Runtime precoding: Enabling multipoint transmission in LTE-advanced system-level simulations." IEEE Access 3 (2015): 725-736.
[18] Jungnickel, Volker, et al. "Backhaul requirements for inter-site cooperation in heterogeneous LTE-Advanced networks." 2013 IEEE International Conference on Communications Workshops (ICC). IEEE, 2013.
[19] Apt, Krzysztof R., and Andreas Witzel. "A generic approach to coalition formation." International Game Theory Review 11.03 (2009): 347-367.